ISPRS Journal of Photogrammetry and Remote Sensing 125 (2017) 125–131

Contents lists available at ScienceDirect

ISPRS Journal of Photogrammetry and Remote Sensing

journal homepage: www.elsevier.com/locate/isprsjprs

Correcting bias in the rational polynomial coefficients of satellite imagery using thin-plate smoothing splines

Xiang Shen [a,b,c], Bin Liu [d], Qing-Quan Li [a,*]

[a] Key Laboratory for Geo-Environmental Monitoring of Coastal Zone of the National Administration of Surveying, Mapping and Geo-Information & Shenzhen Key Laboratory of Spatial-temporal Smart Sensing and Services, Shenzhen University, Nanhai Road 3688, Shenzhen 518060, PR China
[b] Beijing Key Laboratory of Urban Spatial Information Engineering, Beijing 100038, PR China
[c] College of Information Engineering, Shenzhen University, Nanhai Road 3688, Shenzhen 518060, PR China
[d] State Key Laboratory of Remote Sensing Science, Institute of Remote Sensing and Digital Earth (RADI), Chinese Academy of Sciences, Beijing 100101, PR China

ARTICLE INFO

Article history:
Received 6 November 2016
Received in revised form 7 January 2017
Accepted 10 January 2017
Available online 25 January 2017

Keywords:
Rational function model
Satellite photogrammetry
Spline
Systematic error

ABSTRACT

The Rational Function Model (RFM) has proven to be a viable alternative to the rigorous sensor models used for geo-processing of high-resolution satellite imagery. Because of various errors in the satellite ephemeris and instrument calibration, the Rational Polynomial Coefficients (RPCs) supplied by image vendors are often not sufficiently accurate, and there is therefore a clear need to correct the systematic biases in order to meet the requirements of high-precision topographic mapping. In this paper, we propose a new RPC bias-correction method using the thin-plate spline modeling technique. Benefiting from its excellent performance and high flexibility in data fitting, the thin-plate spline model has the potential to remove complex distortions in vendor-provided RPCs, such as the errors caused by short-period orbital perturbations. The performance of the new method was evaluated by using Ziyuan-3 satellite images and was compared against the recently developed least-squares collocation approach, as well as the classical affine-transformation and quadratic-polynomial based methods. The results show that the accuracies of the thin-plate spline and the least-squares collocation approaches were better than the other two methods, which indicates that strong non-rigid deformations exist in the test data because they cannot be adequately modeled by simple polynomial-based methods. The performance of the thin-plate spline method was close to that of the least-squares collocation approach when only a few Ground Control Points (GCPs) were used, and it improved more rapidly with an increase in the number of redundant observations. In the test scenario using 21 GCPs (some of them located at the four corners of the scene), the correction residuals of the thin-plate spline method were about 36%, 37%, and 19% smaller than those of the affine transformation method, the quadratic polynomial method, and the least-squares collocation algorithm, respectively, which demonstrates that the new method can be more effective at removing systematic biases in vendor-supplied RPCs.

1. Introduction

The georeferencing of high-resolution satellite imagery can be conducted by two different approaches: the physical sensor model and the generic sensor model (Poli and Toutin, 2012; Zhang et al., 2015). The former approach is directly built on the collinearity condition, which depicts the geometric relationship between image and object coordinates rigorously by exterior and interior orientation parameters as well as some inter-sensor calibration parameters (Jeong and Kim, 2015; Kim and Jeong, 2011). The latter one, which is commonly constructed by a polynomial or a ratio of two polynomials, is a convenient mathematical approximation to the physical sensor model (Fraser et al., 2006; Fraser and Yamakawa, 2004; Shaker, 2008). The advantage of using a generic rather than a physical sensor model is that its geometric form is independent of the distinct characteristics of different sensors, which facilitates the data processing of high-resolution satellite imagery (Toutin, 2011). In addition, all the technical details relating to cameras and satellite orbits can be safely concealed, which is demanded by some commercial satellite image vendors (Zhang et al., 2015).

The Rational Function Model (RFM), which is defined as a ratio of two cubic polynomials, is currently the most popular generic

* Corresponding author.
E-mail address: liqq@szu.edu.cn (Q.-Q. Li).

http://dx.doi.org/10.1016/j.isprsjprs.2017.01.007
0924-2716/

sensor model used in the field. A great number of researches have reported that the RFM can be utilized for high-precision geopositioning of pushbroom satellite images (Aguilar et al., 2012; Alkan et al., 2013; Di et al., 2003b; Fraser et al., 2006; Poli and Toutin, 2012; Tao and Hu, 2001b), and it can also replace physical sensor models in the data processing of satellite SAR (Synthetic Aperture Radar) (Sekhar et al., 2014; Toutin, 2012; Zhang et al., 2010, 2012a, 2011) and aerial frame photographs (Ma, 2013).

Limited by the inaccurate measurement of satellite orbits and attitudes, the Rational Polynomial Coefficients (RPCs) provided by image vendors are often biased, and the resulting errors in the image space typically range from several pixels to tens of pixels (Jiang et al., 2015; Nagasubramanian et al., 2007; Teo, 2011). The bias correction of vendor-provided RPCs is therefore required in the photogrammetric processing of high-precision satellite images, and it has been continuously studied almost since the RFM was introduced to the remote sensing community (Di et al., 2003a; Fraser and Hanley, 2003; Hong et al., 2015; Tong et al., 2010).

A large number of studies have been conducted to correct the bias in vendor-provided RPCs. Almost all previous methods employ lower-order polynomials in error modeling. Some popular bias models in the literature are the translation model, the shift and drift model, the conformal transformation model, the affine transformation model, and the quadratic polynomial (i.e., the second-order polynomial) model (Fraser and Hanley, 2005; Teo, 2011; Topan, 2013; Wang et al., 2005; Xiong and Zhang, 2009). Many researchers have compared these models using a variety of high-resolution satellite imageries, such as QuickBird (Hong et al., 2015; Tong et al., 2010; Xiong and Zhang, 2011), IKONOS (Grodecki and Dial, 2003; Wang et al., 2005), IRS-P6 (Nagasubramanian et al., 2007), KOMPSAT-2 (Jeong and Kim, 2015), GeoEye-1 (Aguilar et al., 2012, 2013), and WorldView-1/2 (Alkan et al., 2013; Teo, 2011), and most of them have reported that the affine transformation model commonly yields the best performance and the quadratic polynomial model can obtain comparable results when sufficient Ground Control Points (GCPs) are available. Given that the field survey of GCPs is inherently laborious and time consuming, researchers have also developed some cost-efficient algorithms that adopt other reference data, such as topographic maps (Oh and Lee, 2015) and digital elevation models (Oh and Jung, 2016).

Although lower-order polynomial based models have been demonstrated to be capable of efficiently correcting systematic errors in vendor-provided RPCs, there is still plenty of room to further improve the accuracy. In a very recent work, Li et al. (2014) introduced the least-squares collocation algorithm to tackle the RPC bias-correction problem. Their results showed that strong spatially-correlated errors existed in the RPC data of QuickBird, and the least-squares collocation method performed much better than the affine transformation and the quadratic polynomial methods in terms of accuracy and reliability.

In this paper, we propose an alternative approach for the bias correction of RPCs by using the thin-plate spline technique. The thin-plate spline is known as a powerful tool for modeling irregular deformations specified by point correspondences, and it has been applied successfully in a variety of image processing and computer vision applications, e.g., image warping and non-rigid image registration (Bookstein, 1989; Rohr et al., 2001; Ross and Nadgir, 2008; Sotiras et al., 2013). As a nonparametric model, the thin-plate smoothing spline is more powerful and flexible than parametric polynomial models in data fitting (Wahba, 1990), which benefits accurate correction of complex RPC distortions caused by orbit perturbations and other related factors.

The remainder of this paper is organized as follows. Section 2 first gives some basic concepts of the RFM. Then, Section 3 introduces the construction of the thin-plate spline model and the formulas for estimating the smoothing parameter. Finally, we provide experimental results and analysis in Section 4 and conclude our work in the last section.

2. The rational function model

The rational function model describes the geometric relationship between a ground point and its corresponding image point through a ratio of two cubic polynomials (Fraser et al., 2006; Tao and Hu, 2001a; Zhang et al., 2012b). Its general form is defined as

$$\begin{aligned} y_n &= \frac{P_1(\varphi_n,\lambda_n,h_n)}{P_2(\varphi_n,\lambda_n,h_n)} \\ x_n &= \frac{P_3(\varphi_n,\lambda_n,h_n)}{P_4(\varphi_n,\lambda_n,h_n)} \end{aligned} \tag{1}$$

where $(\varphi_n, \lambda_n, h_n)$ refer to the normalized latitude, longitude, and height of a ground point, respectively; (x_n, y_n) are the normalized sample and line coordinates of the corresponding image point, respectively; P_1, P_2, P_3 and P_4 represent third-order polynomials.

The RPCs provided by image vendors are directly derived from satellite ephemeris and attitude data by using the terrain-independent method (Fraser and Hanley, 2003; Li et al., 2014). Limited by the imperfect performance of navigation sensors, the vendor-supplied RPCs are often systematically biased. The most commonly-used and effective solution for bias compensation is to add some corrections to the image coordinates (Hong et al., 2015; Teo, 2011; Wang et al., 2005). In almost all previous studies, the corrections are modeled by a low-order polynomial of the image coordinates, e.g., the translation model (using a zero-order polynomial) and the affine transformation model (using a first-order polynomial).

3. The thin-plate smoothing spline model

The Thin-Plate Spline (TPS) has been widely used in image warping and other image processing operations that require the modeling of non-rigid deformations (Bookstein, 1989; Sotiras et al., 2013). In this paper, we introduce the thin-plate spline technique to solve the RPC bias-correction problem. The following parts of this section provide the details of the TPS algorithm.

3.1. Constructing a thin-plate spline

The general form of the TPS function is given by (SAS Institute Inc., 2015; Wahba, 1990)

$$f(x,y) = \alpha[x \quad y \quad 1]^T + \sum_{j=1}^{m}\delta_j\psi(r_j) \tag{2}$$

with r_j the Euclidean distance

$$r_j = \sqrt{(x-x_j)^2 + (y-y_j)^2} \tag{3}$$

and $\psi()$ the Radial-Basis-Function (RBF) kernel

$$\psi(r) = r^2\log(r^2) \tag{4}$$

where (x, y) are the coordinates of an arbitrary point in the image space, (x_j, y_j) are the measured image coordinates of the jth GCP, m is the number of GCPs, and α and $\delta = (\delta_1, \delta_2, \ldots, \delta_m)$ are the coefficients (row vectors) that need to be estimated by minimizing the following quantity (Green and Silverman, 1993; Wood, 2003).

$$E(f) + \lambda R(f) \tag{5}$$

with $E(f)$ the error measure

$$E(f) = \sum_{j=1}^{m}\|z_j - f(x_j,y_j)\|^2 \tag{6}$$

and $R(f)$ the roughness measure

$$R(f) = \iint \left(\left(\frac{\partial^2 f}{\partial^2 x^2} \right)^2 + 2 \left(\frac{\partial^2 f}{\partial x \partial y} \right)^2 + \left(\frac{\partial^2 f}{\partial^2 y^2} \right)^2 \right) \mathrm{d}x\mathrm{d}y \tag{7}$$

where z_j is the observation (for the RPC bias-correction problem, it refers to the line or sample component of the image-projection error) at (x_j, y_j), and λ is the smoothing parameter (the value is restricted to be non-negative) which controls the smoothness of the allowable deformation. In the case of $\lambda = 0$, there is no smoothness constraints, and the data points are interpolated by the TPS function. If $\lambda = +\infty$, the coefficients δ in Eq. (2) will be an array of zeros, and the TPS function will reduce to an affine transformation model (Mathworks Inc., 2016).Unlike low-order polynomials, a TPS model can describe RPC errors in a flexible way by adjusting the smoothing parameter λ. When only linear errors exist in RPC data, an affine transformation model is suitable for the bias compensation, and a TPS model can yield similar correction results with using a large λ. The RPC data of some satellite images may contain complex deformations caused by short-period orbital perturbations or other factors. An important proportion of the errors are commonly non-rigid, and they can be effectively modeled by a thin-plate spline with a small λ, while low-order polynomials do not have such a capacity. A proper estimation of the smoothing parameter λ is of great importance for the TPS modeling method, and it will be discussed in the next subsection.Supposing λ is known, the coefficients in the TPS function of Eq. (2) can be computed by (Green and Silverman, 1993)

$$\delta = zQ_2[Q_2^T(K + \lambda I_m)Q_2]^{-1}Q_2^T \tag{8}$$

and

$$\alpha = [z - \delta(K + \lambda I_m)]Q_1(R^T)^{-1} \tag{9}$$

where I_m represents the square identity matrix of order m, and the matrices Q_1, Q_2, and R are derived by the QR decomposition of the following matrix.

$$\begin{bmatrix} x_1 & y_1 & 1 \\ x_2 & y_2 & 1 \\ \vdots & \vdots & \vdots \\ x_m & y_m & 1 \end{bmatrix} = \begin{pmatrix} Q_1 & Q_2 \end{pmatrix} \begin{pmatrix} R \\ 0 \end{pmatrix} \tag{10}$$

The matrix K in Eqs. (8) and (9) is formulated as

$$K = \begin{bmatrix} 0 & \psi(r_{1,2}) & \dots & \psi(r_{1,m}) \\ \psi(r_{2,1}) & 0 & \dots & \psi(r_{2,m}) \\ \vdots & \vdots & \ddots & \vdots \\ \psi(r_{m,1}) & \psi(r_{m,2}) & \dots & 0 \end{bmatrix} \tag{11}$$

where $r_{i,j}$ is the Euclidean distance between the two different GCPs.

$$r_{i,j} = \sqrt{(x_i - x_j)^2 + (y_i - y_j)^2} \tag{12}$$

3.2. Estimating the smoothing parameter

The most critical issue in the TPS modeling is to estimate the smoothing parameter λ (Wahba, 1990). Our algorithm adopts the widely-used Generalized Cross-Validation (GCV) criterion, which chooses the smoothing parameter that minimizes the GCV score (Arlot and Celisse, 2010; Garcia, 2010; Ruppert et al., 2003; Wahba, 1990).

$$\hat{\lambda} = \arg\min_{\lambda} \mathrm{GCV}(\lambda) \tag{13}$$

with

$$\mathrm{GCV}(\lambda) = \frac{mRSS_\lambda}{[m - \mathrm{tr}(A_\lambda)]^2} \tag{14}$$

where RSS_λ is the residual sum of squares when using λ in the model fitting, and the function tr() returns the sum of the diagonal elements of the influence matrix A_λ (SAS Institute Inc., 2015).

$$A_\lambda = I_m - \lambda Q_2[Q_2'(K + \lambda I_m)Q_2]^{-1}Q_2' \tag{15}$$

The GCV can be regarded as an approximation to the leave-one-out cross validation (Arlot and Celisse, 2010), and it is not very robust if there are not many redundant observations. To tackle the problem, our algorithm employs the following conservative formula to estimate the smoothing parameter when the number of GCPs is less than the threshold (it was set to 11 in our experiments).

$$\hat{\lambda} = \mathrm{mean}(\mathrm{diag}(Q_2^T K Q_2)) \tag{16}$$

where the function diag() gets diagonal elements of a matrix. This approach has been implemented in the "tpaps" function of the MATLAB curve fitting toolbox (Mathworks Inc., 2016).

4. Experiments

The following four bias-correction methods were chosen for the comparative analysis.

(1) The affine transformation model (AT). It is the most commonly used method in the literature.
(2) The quadratic polynomial model (QP). It refers to the second-order polynomial based method (Hong et al., 2015; Tong et al., 2010) and can be seen as an extended form of the affine transformation model.
(3) The least-squares collocation algorithm (LSC). This method has been widely used in geodesy and was introduced by Li et al. (2014) to solve the RPC bias-correction problem.
(4) The thin-plate spline model (TPS). This is the new approach proposed in this paper.

4.1. Data

The high-resolution image data used in the experiments were captured by the Ziyuan-3 satellite, which was the first civilian three-line-array stereo-mapping satellite launched by China (Pan et al., 2013; Zhang et al., 2015). A stereo triplet of panchromatic images acquired on February 23, 2012 was used for the test, and their basic properties are listed in Table 1. As shown in Fig. 1, the survey area, which is located in the Fangshan District of Beijing, China, covers both urban and mountainous regions. The terrain elevations range from near 0 m to about 1500 m above sea level.

A total of 30 regularly-distributed ground points, as shown in Fig. 1, were collected by GPS field surveys with centimeter-level accuracy. Their corresponding image coordinates were carefully measured by manual means. In the experiments, 30% of ground

Table 1
Characteristics of the stereo images used in the experiments.

Specification	Nadir image	Backward image	Forward image
View angle (deg)	0	−22	22
Ground sample distance (m)	2.08	3.38	3.38
Width (pixels)	24,516	16,306	16,306
Height (pixels)	24,576	16,384	16,384

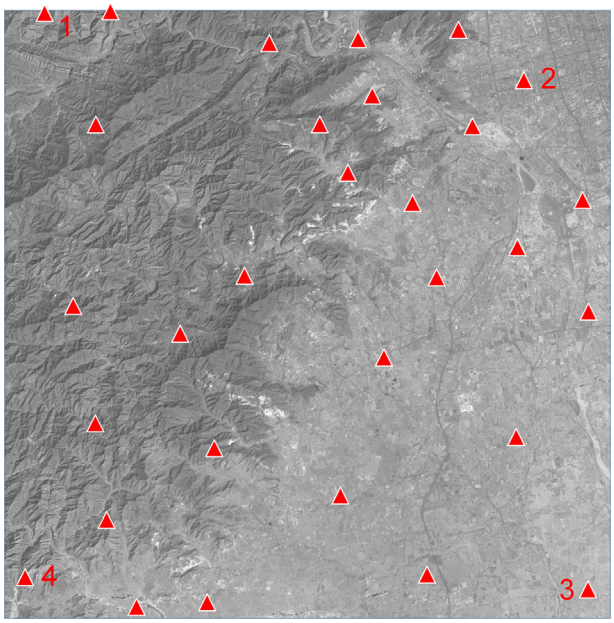

Fig. 1. Ground survey points overlaid on the nadir-view image.

survey points were used as independent check points to assess the accuracy of the four RPC bias-correction methods. Some or all of the remaining ground survey points were employed as GCPs, the number of these ranging from 4 to 21 per test (i.e., 70% of the 30 ground survey points).

4.2. GCP configuration schemes

The following GCP configuration schemes were employed in the experiments:

(1) Four corner GCPs were fixed. The four points located at the corners of the scene (cf. the numbered points in Fig. 1) always served as ground control points, and other GCPs were allocated at random. This scheme, Scheme 1, simulates a relatively regular distribution of GCPs.
(2) No GCPs were fixed. All GCPs were randomly selected from the 30 ground survey points. This scenario, Scheme 2, was used for further testing the stability of the proposed algorithm by simulating unsatisfactory distributions of GCPs, which can happen when some regions of the survey area are inaccessible.
(3) The tests for both Scheme 1 and 2, for a given number of GCPs, were repeated 1000 times, the combination of control points changing each time, and the average performance was calculated for comparison purposes.

4.3. Results

4.3.1. Scheme 1

The experimental results show that the direct georeferencing errors of all the three images exceeded 10 pixels in the image space (i.e., the image-projection errors when the vendor-provided RPCs were directly used in the georeferencing and no bias compensation was performed). In most of the test scenarios, all bias-correction methods successfully reduced the georeferencing residuals to about 1 pixel. As illustrated in Fig. 2, the accuracy of the affine transformation model slightly improved with increases in the number of GCPs, which implies that it barely had the capacity to compensate complex errors in RPCs. The correction residuals of

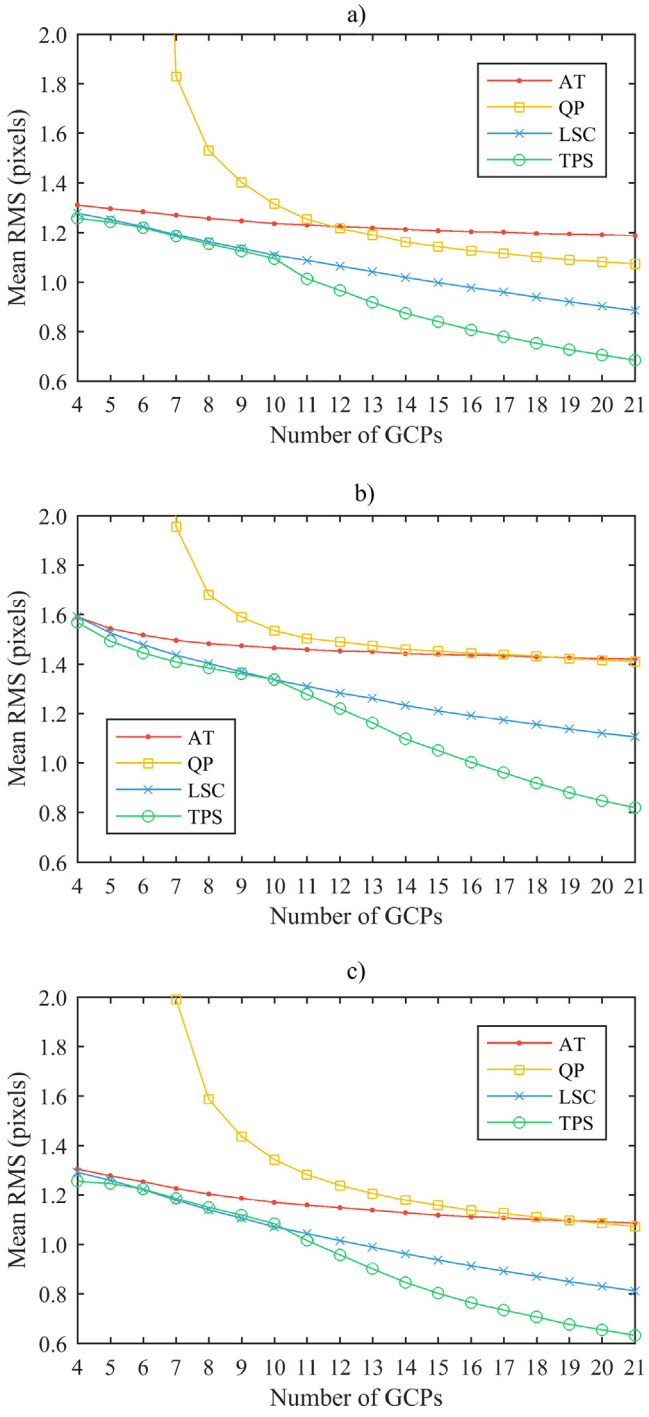

Fig. 2. Statistical results for bias-correction residuals in image space for (a) nadir, (b) backward and (c) forward looking images, with AT being affine, QP the quadratic polynomial, LSC the least-squares collocation and TPS the thin-plate spline model.

the quadratic polynomial model were unacceptably high when only a moderate number of GCPs, around 10 or less, were used. Although the performance of the quadratic polynomial correction method greatly improved when larger numbers of GCPs were used, it was only moderately better than (for the nadir-view image, cf. Fig. 2a) or close to (for the backward- and forward-view images, cf. Fig. 2b and Fig. 2c) that of the affine transformation model. Comparing the results of the four bias-correction methods, it can be concluded that strong non-rigid distortions existed in the test RPCs, because the correction residuals of simple polynomial based

methods (i.e., the AT and QP models) were significantly larger than the other two methods. In the test scenarios where only a few GCPs were employed, the performance of the least-squares collocation algorithm and the thin-plate spline method was very similar. The correction residuals of the thin-plate spline method decreased more rapidly with the addition of redundant control point observations, which proved that it was more effective than the least-squares collocation method in terms of reducing systematic errors in the RPCs.

As shown in Fig. 3, the bias-correction results in object space confirmed the above analysis. The quadratic polynomial method always performed the worst among the four bias-correction methods. When only the four corner GCPs were used, the average correction residuals of the affine transformation, least-squares collocation and thin-plate spline methods were at the same level. With an increase in the number of GCPs, the residuals of the affine transformation method slowly decreased, and for the other two methods, the rate of reduction in the magnitude of the residuals was much faster. In the test scenario that used 21 GCPs, the accuracy of the thin-plate spline method was 36%, 37%, and 19% better than that of the affine transformation, quadratic polynomial and least-squares collocation methods, respectively. Comparing Fig. 3a and b, it can be seen that the reduction in the magnitude of residuals from the thin-plate spline method was more obvious in the planimetric coordinates than in the height component.

The practical performance of a RPC bias-correction method is partly determined by the spatial distribution of GCPs, especially when insufficient GCPs are available. The reliability is, therefore, also a determining factor for comparing different algorithms. In the experiments, the relative reliability was defined through the probability of the accuracy improvement for a RPC bias-correction method with respect to a reference case, and it is calculated by

$$P_{A,B} = \frac{1}{N}\sum_{i=1}^{N} b_{A,B}^{i} \tag{17}$$

with

$$b_{A,B}^{i} = \begin{cases} 1, & \text{if } RMS_A^i < RMS_B^i \\ 0, & \text{otherwise} \end{cases} \tag{18}$$

where N refers to the number of trials (the value is 1000 in the experiments), the RMS values were calculated from three-dimensional errors in the object space, the superscript i refers to the i-th test, and the subscripts A and B represent two different bias-correction methods. When $P_{A,B} > 0.5$, it means that the method A has a higher probability to yield better results than the method B.

Fig. 4 illustrates some major results of the relative reliability between different bias-correction methods. It can be easily seen that the quadratic polynomial model was more likely to yield worse results as compared to the affine model, while the least-squares collocation algorithm and the thin-plate spline method performed significantly better than the affine transformation method in terms of reliability. In the test scenarios of using 8–10

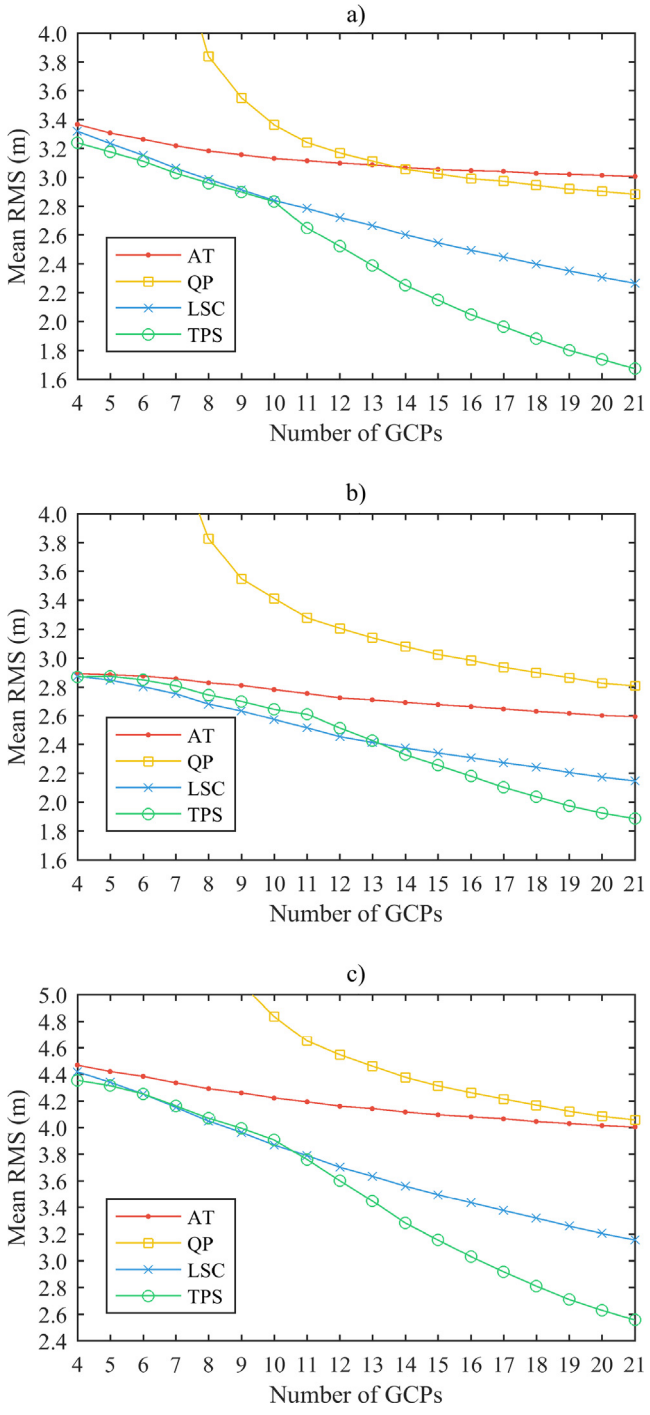

Fig. 3. Statistical results for bias-correction residuals in object space for (a) planimetry, (b) height and (c) three-dimensional errors.

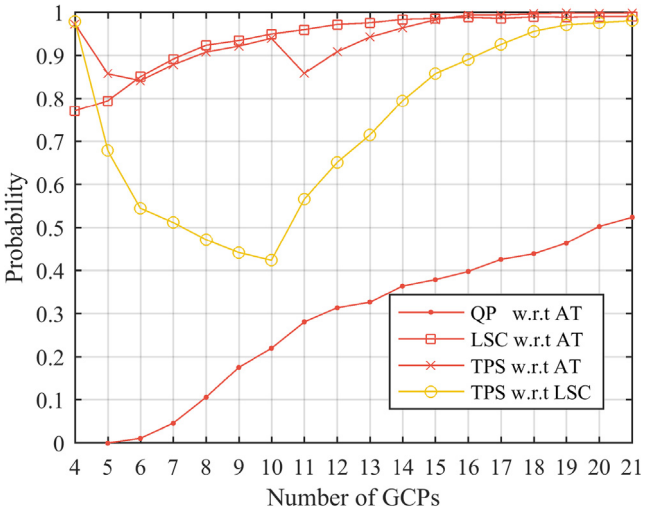

Fig. 4. The probability of accuracy improvement for a test bias-correction method with respect to (w.r.t.) a reference case.

GCPs, the reliability performance of the thin-plate spline method was slightly worse than that of the least-squares collocation algorithm, but in other scenarios, the proposed method yielded much higher probability values.

4.3.2. Scheme 2

Fig. 5 shows the experimental results of Scheme 2. To facilitate the comparison, some outcomes of Scheme 1 are also plotted in the figure. It can be seen from Fig. 5a that imperfect GCP distributions severely degraded the performance of all bias-correction methods, especially when redundant control point observations were limited in number. In the test scenario of using 4 random GCPs, the correction residuals of the affine transformation, least-squares collocation and thin-plate spline methods were all about 72% larger than those in the corresponding scenario of using the corner GCPs. As the number of redundant control point observations increased, the performance difference between the two GCP configuration schemes gradually decreased for all bias-correction methods. In the scenario that utilised 21 GCPs, the accuracy of the thin-plate spline method was 33%, 40%, and 18% better than that of the affine transformation, quadratic polynomial and least-squares collocation methods, respectively, the results being very close to those of Scheme 1 (cf. Section 4.3.1).

Finally, as shown in Fig. 5b, the relative reliability of the thin-plate spline method as compared to other bias-correction methods

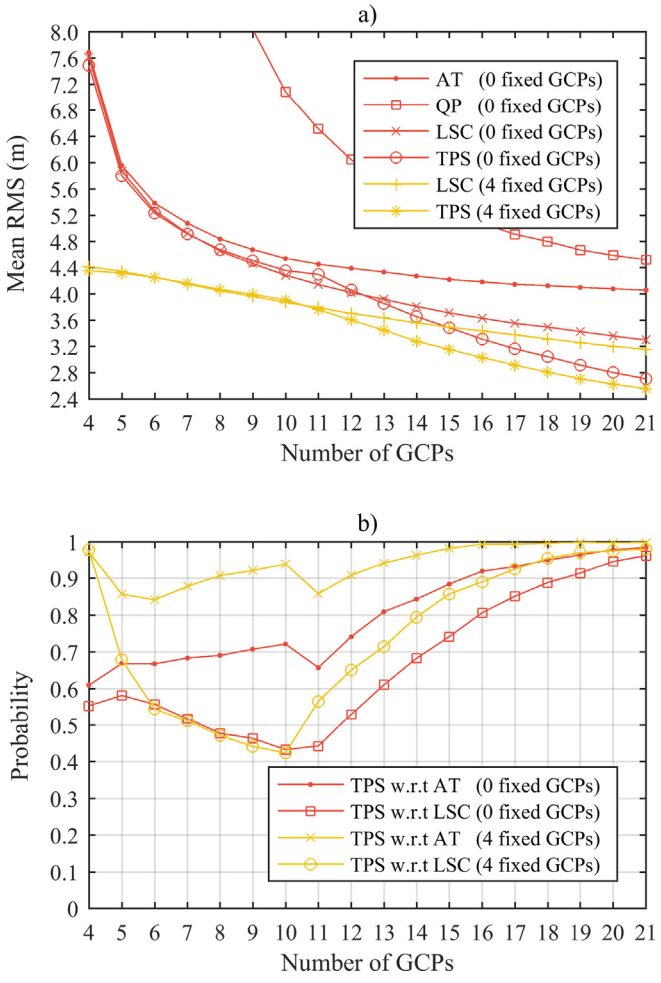

Fig. 5. Comparison between the experimental results of the two GCP configuration schemes: (a) three-dimensional residuals of bias correction, and (b) probability of accuracy improvement for the thin-plate spline method w.r.t. the least-squares collocation algorithm.

in Scheme 2 was not as high as that for Scheme 1. However, given that the probability of the accuracy improvement still generally exceeded 50%, it can be safely concluded that, in most practical scenarios, the new method has a higher possibility of reducing more biases in vendor-provided RPCs.

4.4. Discussion

Comparative experiments have also been conducted on some IKONOS images and more Ziyuan-3 scenes. No obvious non-rigid errors were detected in these data sets. The correction accuracies for almost all test images have reached 0.5–0.7 pixel even if only four corner GCPs were used, and they have just slightly improved with an increase in the number of GCPs. The performance of the TPS model was very close to that of the affine transformation model. In most test scenarios, the accuracy difference between the two methods was smaller than 0.05 pixel, which shows the applicability of the TPS model on the satellite images with the RPC data only containing linear errors.

5. Conclusions

The geopositioning accuracy of high-resolution satellite imagery can be adversely affected in situations where vendor-supplied RPCs insufficiently model non-rigid image deformations attributable to error sources such as short-period orbital perturbations and imperfect instrument calibration. In this paper, the authors have introduced the thin-plate spline technique to model complex biases in vendor-supplied RPCs, and they have compared its performance to that of three other published bias-correction methods. From the experiments on a stereo triplet of Ziyuan-3 images, the following conclusions can be drawn:

(1) Strong non-rigid distortions exist in the vendor-provided RPCs of the Ziyuan-3 satellite. When sufficient GCPs are available, both the least-squares collocation algorithm and the thin-plate spline method perform much better than simple polynomial-based methods, which indicates that some biases in the test RPC data are local in nature.
(2) The thin-plate spline method is more effective at removing complex RPC biases than the least-squares collocation algorithm. In the test scenario using 21 GCPs, nearly 20% of residuals resulting from the application of the least-squares collocation algorithm could be further reduced in magnitude by the thin-plate spline method.
(3) The performance of the thin-plate spline method is relatively stable. When all GCPs were randomly distributed, the accuracy of all bias-correction methods was, as expected, worse than that in the test scenario where four GCPs in the corners of the scene were fixed. Moreover, the ratio of performance degradation for the thin-plate spline method was at the same level as that for both the affine transformation and the least-squares collocation algorithms.

Acknowledgments

This research was supported by the National Natural Science Foundation of China (Nos. 41601493 and 41301528), the China Postdoctoral Science Foundation (No. 2015M570724), the Beijing Key Laboratory of Urban Spatial Information Engineering (No. 2014206), and the Shenzhen future industry development funding program (No. 20150721121924786O).

References

Aguilar, M.A., Aguilar, F.J., Saldana, M.D., Fernandez, I., 2012. Geopositioning accuracy assessment of GeoEye-1 panchromatic and multispectral imagery. Photogram. Eng. Rem. Sens. 78 (3), 247–257.

Aguilar, M.A., Saldana, M.D., Aguilar, F.J., 2013. Assessing geometric accuracy of the orthorectification process from GeoEye-1 and WorldView-2 panchromatic images. Int. J. Appl. Earth Obs. Geoinf. 21, 427–435.

Alkan, M., Buyuksalih, G., Sefercik, U.G., Jacobsen, K., 2013. Geometric accuracy and information content of WorldView-1 images. Opt. Eng. 52 (2), 026201 (1–7).

Arlot, S., Celisse, A., 2010. A survey of cross-validation procedures for model selection. Stat. Surv. 4, 40–79.

Bookstein, F.L., 1989. Principal warps: thin-plate splines and the decomposition of deformations. IEEE Trans. Pattern Anal. Mach. Intell. 11 (6), 567–585.

Di, K., Ma, R., Li, R., 2003a. Geometric processing of Ikonos stereo imagery for coastal mapping applications. Photogram. Eng. Rem. Sens. 69 (8), 873–879.

Di, K., Ma, R., Li, R., 2003b. Rational functions and potential for rigorous sensor model recovery. Photogram. Eng. Rem. Sens. 69 (1), 33–41.

Fraser, C.S., Dial, G., Grodecki, J., 2006. Sensor orientation via RPCs. ISPRS J. Photogram. Rem. Sens. 60 (3), 182–194.

Fraser, C.S., Hanley, H.B., 2003. Bias compensation in rational functions for Ikonos satellite imagery. Photogram. Eng. Rem. Sens. 69 (1), 53–57.

Fraser, C.S., Hanley, H.B., 2005. Bias-compensated RPCs for sensor orientation of high-resolution satellite imagery. Photogram. Eng. Rem. Sens. 71 (8), 909–915.

Fraser, C.S., Yamakawa, T., 2004. Insights into the affine model for high-resolution satellite sensor orientation. ISPRS J. Photogram. Rem. Sens. 58 (5–6), 275–288.

Garcia, D., 2010. Robust smoothing of gridded data in one and higher dimensions with missing values. Comput. Stat. Data Anal. 54 (4), 1167–1178.

Green, P.J., Silverman, B.W., 1993. Nonparametric Regression and Generalized Linear Models: A Roughness Penalty Approach. Chapman & Hall, London.

Grodecki, J., Dial, G., 2003. Block adjustment of high-resolution satellite images described by rational polynomials. Photogram. Eng. Rem. Sens. 69 (1), 59–68.

Hong, Z.H., Tong, X.H., Liu, S.J., Chen, P., Xie, H., Jin, Y.M., 2015. A comparison of the performance of bias-corrected RSMs and RFMs for the geo-positioning of high-resolution satellite stereo imagery. Rem. Sens. 7 (12), 16815–16830.

Jeong, J., Kim, T., 2015. Comparison of positioning accuracy of a rigorous sensor model and two rational function models for weak stereo geometry. ISPRS J. Photogram. Rem. Sens. 108, 172–182.

Jiang, Y.H., Zhang, G., Chen, P., Li, D.R., Tang, X.M., Huang, W.C., 2015. Systematic error compensation based on a rational function model for ziyuan1-02C. IEEE Trans. Geosci. Remote Sens. 53 (7), 3985–3995.

Kim, T., Jeong, J., 2011. DEM matching for bias compensation of rigorous pushbroom sensor models. ISPRS J. Photogram. Rem. Sens. 66 (5), 692–699.

Li, C., Shen, Y.Z., Li, B.F., Qiao, G., Liu, S.J., Wang, W.I., Tong, X.H., 2014. An improved geopositioning model of QuickBird high resolution satellite imagery by compensating spatial correlated errors. ISPRS J. Photogram. Rem. Sens. 96, 12–19.

Ma, R.J., 2013. Rational function model in processing historical aerial photographs. Photogram. Eng. Rem. Sens. 79 (4), 337–345.

Mathworks Inc., 2016. Curve Fitting Toolbox™ User's Guide (Version 3.5.3).

Nagasubramanian, V., Radhadevi, P.V., Ramachandran, R., Krishnan, R., 2007. Rational function model for sensor orientation of IRS-P6 LISS-4 imagery. Photogram. Rec. 22 (120), 309–320.

Oh, J., Lee, C., 2015. Automated bias-compensation of rational polynomial coefficients of high resolution satellite imagery based on topographic maps. ISPRS J. Photogram. Rem. Sens. 100, 14–22.

Oh, K.Y., Jung, H.S., 2016. Automated bias-compensation approach for pushbroom sensor modeling using digital elevation model. IEEE Trans. Geosci. Remote Sens. 54 (6), 3400–3409.

Pan, H.B., Zhang, G., Tang, X.M., Li, D.R., Zhu, X.Y., Zhou, P., Jiang, Y.H., 2013. Basic products of the ZiYuan-3 satellite and accuracy evaluation. Photogram. Eng. Rem. Sens. 79 (12), 1131–1145.

Poli, D., Toutin, T., 2012. Review of developments in geometric modelling for high resolution satellite pushbroom sensors. Photogram. Rec. 26 (137), 58–73.

Rohr, K., Stiehl, H.S., Sprengel, R., Buzug, T.M., Weese, J., Kuhn, M.H., 2001. Landmark-based elastic registration using approximating thin-plate splines. IEEE Trans. Med. Imaging 20 (6), 526–534.

Ross, A., Nadgir, R., 2008. A Thin-Plate Spline Calibration model for fingerprint sensor interoperability. IEEE Trans. Knowl. Data Eng. 20 (8), 1097–1110.

Ruppert, D., Wand, M.P., Carroll, R.J., 2003. Semiparametric Regression. Cambridge University Press, New York.

SAS Institute Inc., 2015. SAS/STAT® 14.1 User's Guide: The TPSPLINE procedure.

Sekhar, K.S.S., Kumar, A.S., Dadhwal, V.K., 2014. Geocoding RISAT-1 MRS images using bias-compensated RPC models. Int. J. Remote Sens. 35 (20), 7303–7315.

Shaker, A., 2008. Satellite sensor modeling and 3D geo-positioning using empirical models. Int. J. Appl. Earth Obs. Geoinf. 10 (3), 282–295.

Sotiras, A., Davatzikos, C., Paragios, N., 2013. Deformable medical image registration: a survey. IEEE Trans. Med. Imaging 32 (7), 1153–1190.

Tao, C.V., Hu, Y., 2001a. A comprehensive study of the rational function model for photogrammetric processing. Photogram. Eng. Rem. Sens. 67 (12), 1347–1357.

Tao, C.V., Hu, Y., 2001b. Use of the rational function model for image rectification. Can. J. Rem. Sens. 27 (6), 593–602.

Teo, T.A., 2011. Bias compensation in a rigorous sensor model and rational function model for high-resolution satellite images. Photogram. Eng. Rem. Sens. 77 (12), 1211–1220.

Tong, X.H., Liu, S.J., Weng, Q.H., 2010. Bias-corrected rational polynomial coefficients for high accuracy geo-positioning of QuickBird stereo imagery. ISPRS J. Photogram. Rem. Sens. 65 (2), 218–226.

Topan, H., 2013. First experience with figure condition analysis aided bias compensated rational function model for georeferencing of high resolution satellite images. J. Indian Soc. Rem. Sens. 41 (4), 807–818.

Toutin, T., 2011. State-of-the-art of geometric correction of remote sensing data: a data fusion perspective. Int. J. Image Data Fusion 2 (1), 3–35.

Toutin, T., 2012. Radarsat-2 DSM generation with new hybrid, deterministic, and empirical geometric modeling without GCP. IEEE Trans. Geosci. Remote Sens. 50 (5), 2049–2055.

Wahba, G., 1990. Spline Models for Observational Data. Society for Industrial and Applied Mathematics, Philadelphia.

Wang, J., Di, K.C., Li, R., 2005. Evaluation and improvement of geopositioning accuracy of IKONOS stereo imagery. J. Surv. Eng. (ASCE) 131 (2), 35–42.

Wood, S.N., 2003. Thin plate regression splines. J. Roy. Stat. Soc. Ser. B (Stat. Method.) 65 (Part 1), 95–114.

Xiong, Z., Zhang, Y., 2009. A generic method for RPC refinement using ground control information. Photogram. Eng. Rem. Sens. 75 (9), 1083–1092.

Xiong, Z., Zhang, Y., 2011. Bundle adjustment with rational polynomial camera models based on generic method. IEEE Trans. Geosci. Remote Sens. 49 (1), 190–202.

Zhang, G., Fei, W.B., Li, Z., Zhu, X.Y., Li, D.R., 2010. Evaluation of the RPC model for spaceborne SAR imagery. Photogram. Eng. Rem. Sens. 76 (6), 727–733.

Zhang, L., Balz, T., Liao, M., 2012a. Satellite SAR geocoding with refined RPC model. ISPRS J. Photogram. Rem. Sens. 69, 37–49.

Zhang, L., He, X., Balz, T., Wei, X., Liao, M., 2011. Rational function modeling for spaceborne SAR datasets. ISPRS J. Photogram. Rem. Sens. 66 (1), 133–145.

Zhang, Y., Zheng, M., Xiong, X., Xiong, J., 2015. Multistrip bundle block adjustment of ZY-3 satellite imagery by rigorous sensor model without ground control point. IEEE Geosci. Remote Sens. Lett. 12 (4), 865–869.

Zhang, Y., Lu, Y., Wang, L., Huang, X., 2012b. A new approach on optimization of the rational function model of high-resolution satellite imagery. IEEE Trans. Geosci. Remote Sens. 50 (7), 2758–2764.